Investigation and Analysis of Harmonics in Different Control Techniques of PMSM Drives: An Application of Power System Health Monitoring

Ritu Tak and Satyendra Singh

Abstract Monitoring of the power system is one of most important accepts in the power grid. Power system monitoring includes the contingency analysis, security concern, optimal operation and the control of the wide area of the power system. Permanent magnet synchronous motor (PMSM) drive scheme is the best choice for the high power application and as a control drive in the power system monitoring. In this chapter, the simulation and modulation of the PMSM drive system have been done and investing or analyzing the presence of the harmonic in torque of the PMSM drive by the different control techniques. Harmonic distortion reduces the performance of the drive, and indirectly, it decreases the reliability of the power system. Basically, torque control method utilizing space and hysteresis vector pulse width modulation in PMSM is compared on the basis of harmonic distortion. The result of analyses shows torque control using a space vector pulse width modulation method is preferred in PMSM for high power applications or for the controlling drives in power system monitoring.

Keywords Torque · Harmonic distortion · Hysteresis current controller · Space vector pulse width modulation · Carrier frequency

1 Introduction

PMSM drives are mostly used as the controller drives in high power application such as in electric vehicles, for motion control system, in rail vehicle drive system because it produces a lot of electricity and is quite efficient as compared to induction motors. In many applications, PMSM drives replace the induction motor drives due to various unique qualities of PMSM [1–3]. In power system monitoring, PMSM drives is preferred as a control drive due to its superior dynamic performance. The existing challenge in the concern of reliability in power system depends on the controlling system of the contemporary area of the power system. In power system monitoring

R. Tak (✉) · S. Singh
School of Electrical Engineering, Bhartiya Skill Development University, Jaipur, India

H. Malik et al. (eds.), *Intelligent Data Analytics for Power and Energy Systems*,
Lecture Notes in Electrical Engineering 802,
https://doi.org/10.1007/978-981-16-6081-8_14

including oscillatory stability monitoring analysis, and control techniques, in this paper analysis the presence of harmonics in different control strategy of PMSM drive [4, 5]. The performance of the controlling drives has an impact on the power system's reliability. The effectiveness of the drive depends upon the technique of controlling torque. The reference current trajectory is specified in the torque control arrangement and the current controller forces the load current to follow it [6, 7]. A comparative analysis of the PMSM with the various control strategies has been done and presented in the chapters [8–10] from the simulation results which show that the optimal torque per ampere control approach outperforms to the opponent. Soft computing and advance intelligent systems and computing technique are used for diagnostics of PMSM drive [11] for improving their performance. The two well-known schemes for current control in the PMSM are hysteresis and PWM technique. In the work [12], the torque control system for a surface-mounted PMSM was simulated and investigated. In articles [13, 14], researchers look into and create a mechanism for tracking torque in PMSM drives using the hysteresis current control approach. For PMSM drives, a three-level hysteresis current control method is presented for decreasing harmonic content [15]. The behavior of the PMSM control drives torque using field weakening scheme is analyzed in chapter [16]. PMSM control drives are most popular in controlling the mechanical or hydraulic system; a new scheme is proposed in chapter [17, 18] for reducing the harmonic level. Artificial intelligence techniques like neural network or fuzzy logic system is used in PMSM controller drives for improving the reliability or reducing the harmonics in the power system [19]; if the reliability of the controlling drives PMSM increases, then indirectly the reliability of the power monitoring system enhances. The scheme of torque and speed control of PMSM drive is analyzed by increasing the speed of the drive about 20–30% of nominal rpm at the condition of field weakened; the experiment result shows in [20, 21].

These below points highlighted the work done in this chapter:

- The design of the model for PMSM control drive has considered.
- The harmonic content has examined when modeling the space vector pulse width modulation (SVPWM) control system of the PMSM drive.
- The hysteresis control system of the PMSM drive has been modeled, and the harmonic content has been examined.
- At a diverse set of working situations such as varying the carrier frequency in SVPWM or vary the current window in the hysteresis control technique has been investigated for the performance of the PMSM control drive.
- The pulsation or the ripple content in the torque and current waveforms by using these two techniques have been analyzed and compared.

Organization of the chapter: Sect. 1 describes the literature review or the importance of control drive in power system monitoring. In Sect. 2, the proposed approach is described by using the flow chart; it explains stepwise the work done in this chapter. The super dynamic model or the mathematical presentation of the physical model of PMSM controller drive is discussed in Sects. 3 and 4. The two most popular control techniques of PMSM drive are explained in Sect. 5. In comparative way, the

harmonic analysis of SVPWM control scheme and hysteresis control scheme are shown in Sect. 6. In Sect. 7, from the result of analyzes, chapter is concluded.

2 Proposed Approach

The flow chart explains the holistic work done in the chapter in the step-by-step manner.

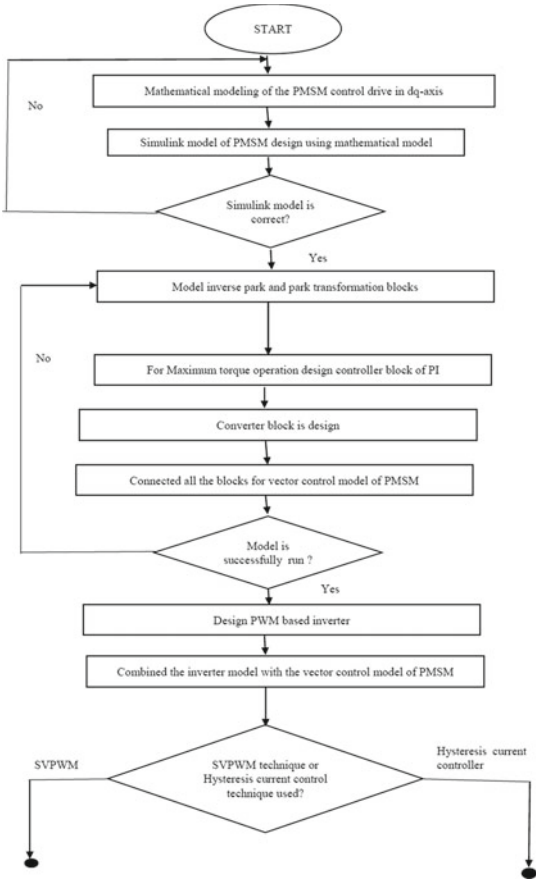

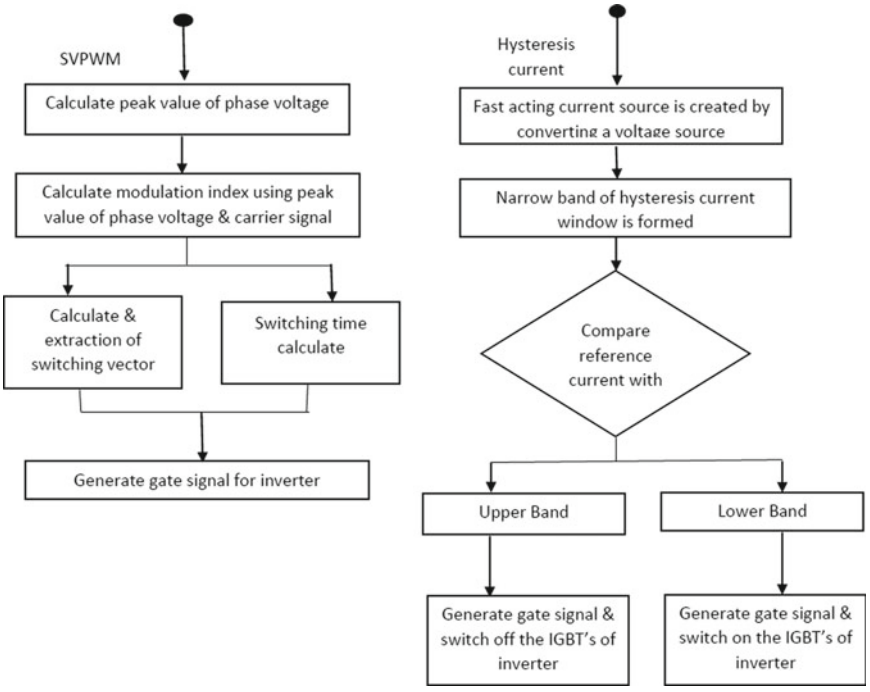

3 Mathematical Derivation of PMSM Drive

The stator voltages and stator flux linkages of the *d*-*q* axis of PMSM drive can be written as [22]:

$$V_{qs} = R_q i_{qs} + \frac{\mathrm{d}}{\mathrm{d}t}\lambda_{qs} \tag{1}$$

$$V_{ds} = R_d i_{ds} + \frac{\mathrm{d}}{\mathrm{d}t}\lambda_{ds} \tag{2}$$

$$\lambda_{qs} = L_{qq} i_{qs} + L_{qd} i_{ds} + \lambda_{af} \sin\theta_{ir} \tag{3}$$

$$\lambda_{ds} = L_{dq} i_{qs} + L_{qd} i_{ds} + \lambda_{af} \cos\theta_{ir} \tag{4}$$

In balanced condition, the resistance of *q*-axis is equal to resistance of *d*-axis. Let it be supposed R_{qd}; the *q*-axis and *d*-axis inductances are also in the surface-mounted PMSM drive; θ_{ir} is the instantaneous rotor situation.

An equation for the voltage of stator in terms of the rotor position is:

$$\begin{bmatrix} V_{qs} \\ V_{ds} \end{bmatrix} = R_s \begin{bmatrix} i_{qs} \\ i_{ds} \end{bmatrix} + \begin{bmatrix} \frac{1}{2}(L_q + L_d) & 0 \\ 0 & \frac{1}{2}(L_q + L_d) \end{bmatrix} \frac{\mathrm{d}}{\mathrm{d}t} \begin{bmatrix} i_{qs} \\ i_{ds} \end{bmatrix} + \lambda_{af}\omega_r \begin{bmatrix} \cos\theta_{ir} \\ -\sin\theta_{ir} \end{bmatrix} \tag{5}$$

The rotor orientation casings are now connected to the stationary orientation edges as follows:

$$i_q d_s = [T^r] i_q^r d_s \tag{6}$$

$$v_q d_s = [T^r] v_q^r d_s \tag{7}$$

$$T^r = \begin{bmatrix} \cos\theta_{ir} & \sin\theta_{ir} \\ -\sin\theta_{ir} & \cos\theta_{ir} \end{bmatrix} \tag{8}$$

$$\begin{bmatrix} v_{qs}^r \\ v_{ds}^r \end{bmatrix} = \begin{bmatrix} R_s + L_q p & \omega_r L_d \\ -\omega_r L_q & R_s + L_d p \end{bmatrix} \begin{bmatrix} i_{qs}^r \\ i_{ds}^r \end{bmatrix} + \begin{bmatrix} \omega_r \lambda_{af} \\ 0 \end{bmatrix} \tag{9}$$

$$\begin{bmatrix} i_{qs}^r \\ i_{ds}^r \\ i_0 \end{bmatrix} = \frac{2}{3} \begin{bmatrix} \cos\theta_{ir} & \cos\left(\theta_{ir} - \frac{2\pi}{3}\right) & \cos\left(\theta_{ir} + \frac{2\pi}{3}\right) \\ \sin\theta_{ir} & \sin\left(\theta_{ir} - \frac{2\pi}{3}\right) & \sin\left(\theta_{ir} + \frac{2\pi}{3}\right) \\ \frac{1}{2} & \frac{1}{2} & \frac{1}{2} \end{bmatrix} \begin{bmatrix} i_{as} \\ i_{bs} \\ i_{cs} \end{bmatrix} \tag{10}$$

4 Scheme of Controlling Torque in PMSM Drive

The stator current that produces flux can be estimated using the current locations and the torque perspective as [23]

$$\begin{bmatrix} i_T^* \\ i_f^* \end{bmatrix} = i_{\text{sref}} \begin{bmatrix} \sin\delta \\ \cos\delta \end{bmatrix} \tag{11}$$

By transformation of *d-q* axis to *abc* axis the references of the phase current are obtained as

$$\begin{bmatrix} i_{as}^* \\ i_{bs}^* \\ i_{cs}^* \end{bmatrix} = \begin{bmatrix} \cos\theta_{ir} & \sin\theta_{ir} \\ \cos\left(\theta_{ir} - \frac{2\pi}{3}\right) & \sin\left(\theta_{ir} - \frac{2\pi}{3}\right) \\ \cos\left(\theta_{ir} + \frac{2\pi}{3}\right) & \sin\left(\theta_{ir} + \frac{2\pi}{3}\right) \end{bmatrix} \begin{bmatrix} i_T^* \\ i_f^* \end{bmatrix} = i_{\text{sref}} \begin{bmatrix} \sin(\theta_{ir} + \delta_{\text{ref}}) \\ \sin\left(\theta_{ir} + \delta_{\text{ref}} - \frac{2\pi}{3}\right) \\ \sin\left(\theta_{ir} + \delta_{\text{ref}} + \frac{2\pi}{3}\right) \end{bmatrix} \tag{12}$$

The proportion integral controller is used to control and make the errors in the phase currents to be zero or yield the reference phase voltage. The reference voltage generated by the PI controller creates the gating indications for the inverter through

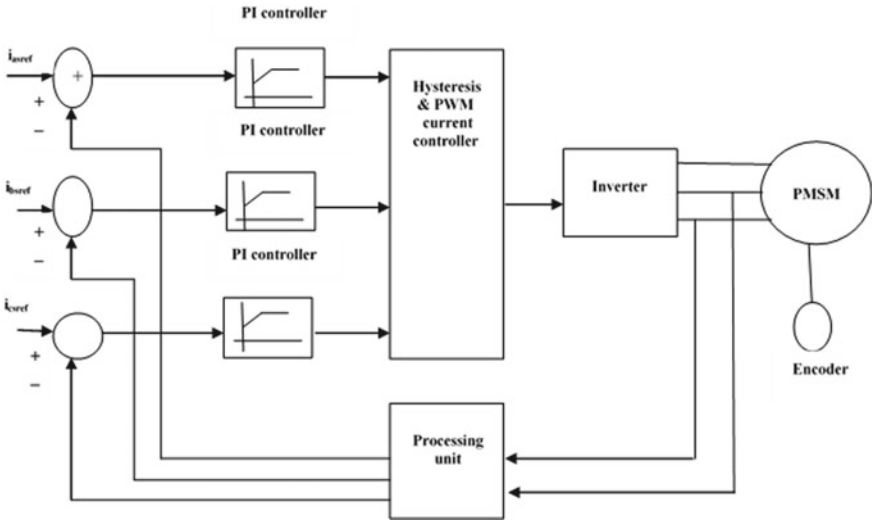

Fig. 1 Torque controlling scheme of PMSM drive

the current controller. The two popular technique hysteresis and SVPWM current controllers are discussed in this chapter.

The schematic flow chart of basic torque design is shown in Fig. 1.

5 Implementation of Controlling Schemes of Torque in PMSM Drive

5.1 Hysteresis Current Controller

A fast-acting current source is produced in the hysteresis controller by translating a voltage source. A small band of excursion is generated from the intended value to regulate the actual current with a hysteresis controller. By summing the stator phase current inside a limited envelope, a hysteresis window is determined and subtracting the preset deviation of current Δi from the stator phase current reference.

As a result, the hysteresis phase current controller's switching logic is as follows:

$$i_{as} - i_{as}^{*} \geq \Delta i \quad \text{set } v_{ao} = \frac{V_{dc}}{2} \tag{13}$$

$$i_{as} - i_{as}^{*} \leq -\Delta i \quad \text{set } v_{ao} = \frac{-V_{dc}}{2}$$

Other stages' implementation can be done in the same way. The voltages on the *d*- and *q*-axes, as well as the stator current, may be calculated using the phase and line voltages. The *d*- and *q*-axis stator currents, as well as torque and mutual flux connections from the rotor reference frames, are used to calculate stator phase currents.

In the hysteresis controller, only the instantaneous peak current and windowed current are dependent on the magnitude of the hysteresis. The hysteresis current controller performance increases with decreasing current windows as the analysis shows.

5.2 SVPWM Current Controller

Harmonics and variations in the fundamental component can be controlled by varying the duration of the useful input voltage. This is achieved by altering the pulse width of the inverter's gate signal, which is known as PWM. There have been several PWM schemes to employ in motor drives. In general, all PWM systems seek to enhance fundamental harmonics while selectively eliminating a few lesser harmonics. The voltage signal generated by the current controller serves as the reference signal for the PWM controller, which interacts with the carrier signal to create gate pulses [24].

The logic of switching for SVPWM to generate the gating signal of inverter as

$$v_{\text{am}} = \frac{V_{\text{dc}}}{2} \frac{v_{\text{pref}}}{v_{\text{pc}}} \tag{14}$$

where

v_{pref} is a phase peak value.
v_{pc} is the carrier signal peak value.

The modulation index of PWM is define as

$$m = \frac{v_{\text{pref}}}{v_{\text{pc}}} \tag{15}$$

By changing the carrier signal, peak value changes modulation index and that changes the amplitude of the fundamental quantity.

6 Analysis of Harmonics in Different Control Techniques of PMSM Drives

The parameter of the PMSM controller drive for analyzing is set to as specified in Table 1.

Table 1 Parameters of PMSM drive

Parameters	Representation	Significance
Rated speed	ω_r	300 rpm
Poles	p	4
q-axis inductance	L_q	0.006 H
Stator resistance	R_s	1.67 Ω
Friction coefficient	B	0.01 Nms
d-axis inductance	L_d	0.0043 H
Inertia moment	J	0.007 kg/m^2
Rotor flux linkage	λaf	0.1400 Wb

The torque-controlled schemes are analyzed for improving the performance of the PMSM drive. Moreover, it enhanced the reliability of the power monitoring arrangement.

6.1 Torque Control Scheme with Hysteresis Current Controller

The response of PMSM is observed with the hysteresis current controller for change in hysteresis current window. The variation of torque, speed, current and flux linkage are analyzed for different values of hysteresis current window. The THD levels of the phase current in PMSM compare with different values of the hysteresis current window.

Figure 2 shows the reaction of the PMSM drive with a constant velocity of 314 rad/s is preferred as base velocity at the hysteresis band of 0.6 p.u. The parameters are represented in normalized units on the graph (p.u.).

The THD in phase *a* current with the hysteresis band of 0.6 p.u. is shown in Fig. 3 is 20.22%.

The response of PMSM drive with the hysteresis band 2.4 p.u. and its THD spectrum is revealed in Figs. 4 and 5 correspondingly. Similarly, with the hysteresis band 3.6 p.u. the response of PMSM and its THD spectrum is shown in Figs. 6 and 7.

Table 2 gives the comparative analyzes of the THD level in phase current of the PMSM drive by different values of the hysteresis current window.

The torque variation with different values of the hysteresis current window is shown in Fig. 8. The simulation result shows that the hysteresis current window; if narrow, then the pulsation in torque is less, and it follows the reference torque.

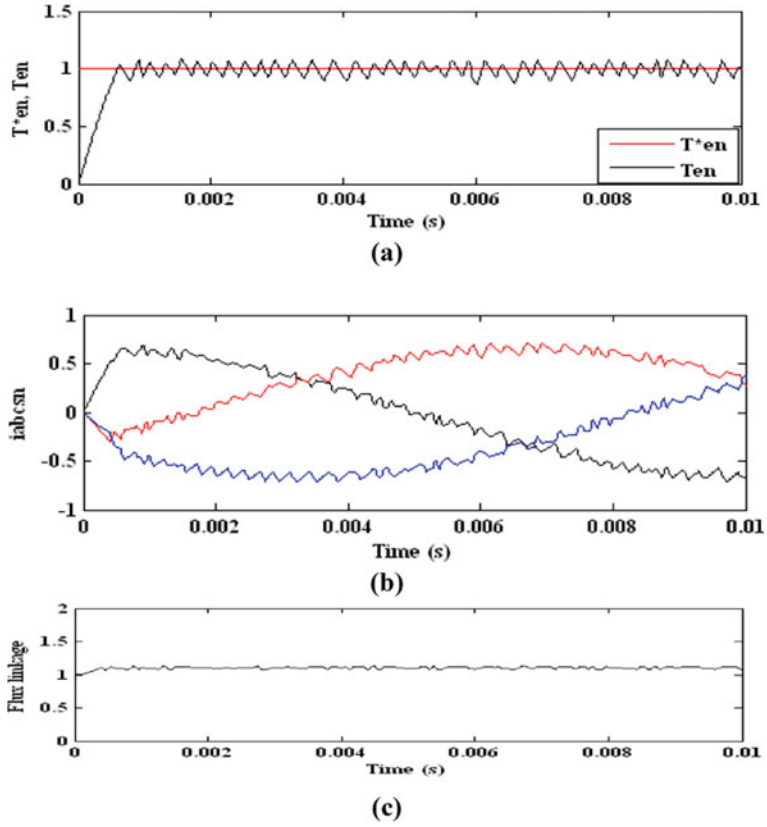

Fig. 2 At hysteresis band of 0.6 p.u. **a** Response for torque, **b** response for phase current, **c** response for flux

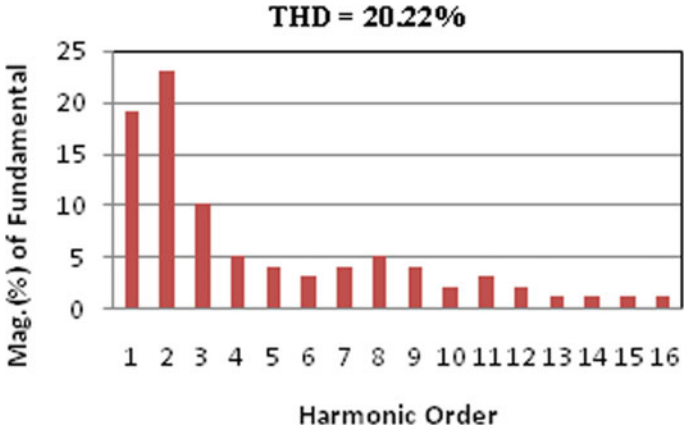

Fig. 3 THD spectrum with hysteresis band 0.6 p.u.

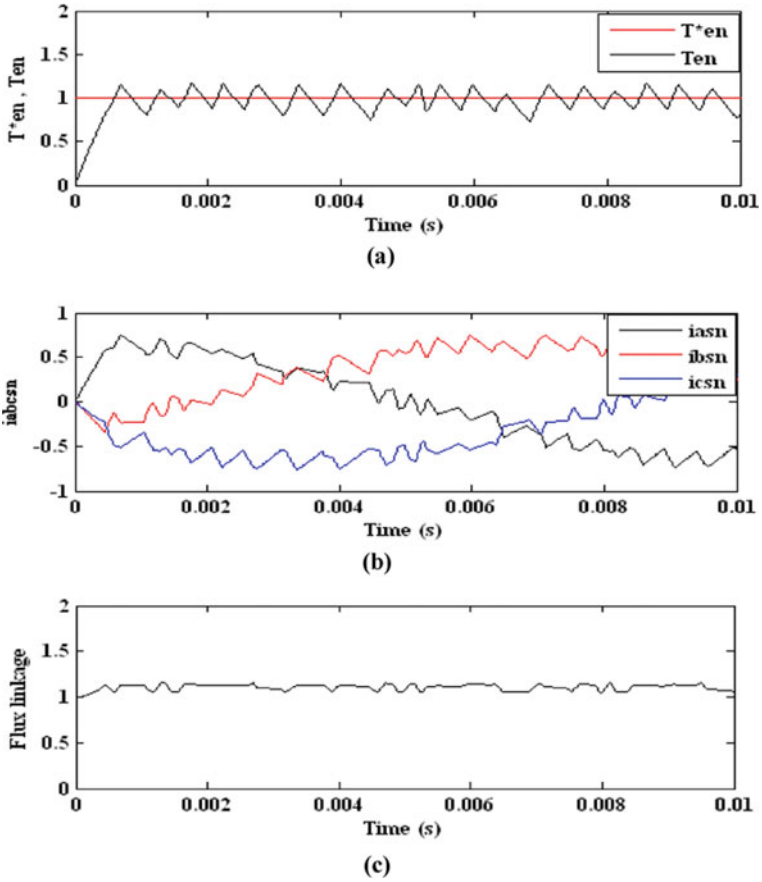

Fig. 4 At hysteresis band of 2.4 p.u. **a** Response for torque, **b** response for phase current, **c** response for flux

Fig. 5 THD spectrum with hysteresis band 2.4 p.u.

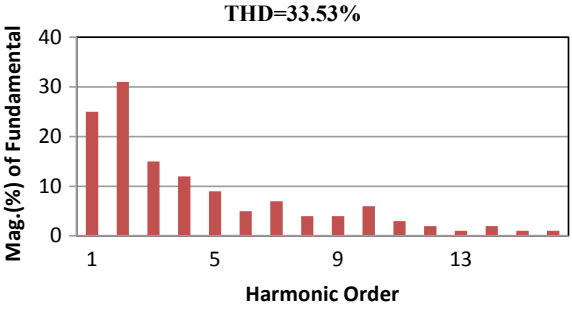

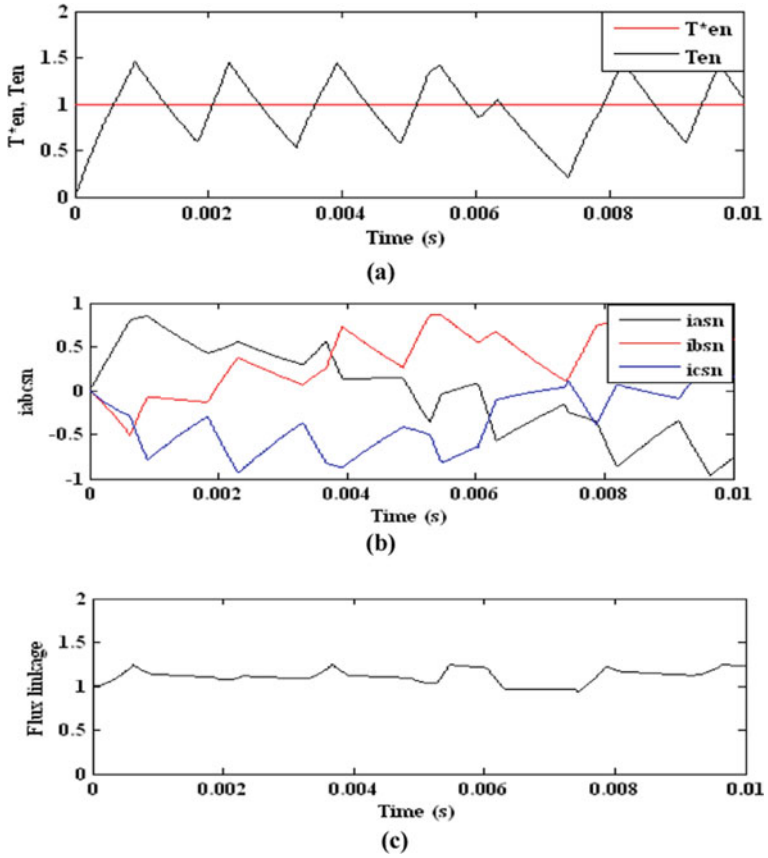

Fig. 6 At hysteresis band of 3.6 p.u. **a** Response for torque, **b** response for phase current, **c** response for flux

Fig. 7 THD spectrum with hysteresis band 3.6 p.u.

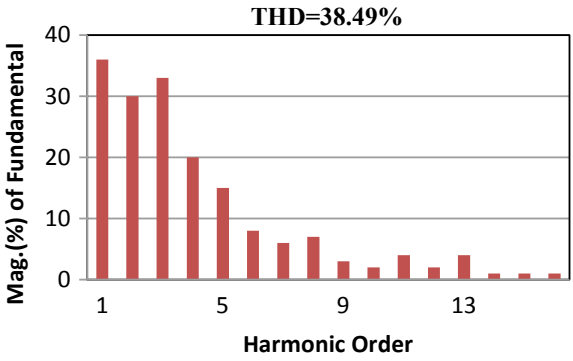

Table 2 Analysis of THD in the current of the PMSM drive with hysteresis current controller

S. No.	Control of hysteresis current	
	Hysteresis band (p.u.)	THD in current %
1	$\Delta i = 0.6$	20.22
2	$\Delta i = 2.4$	33.53
3	$\Delta i = 3.6$	38.49

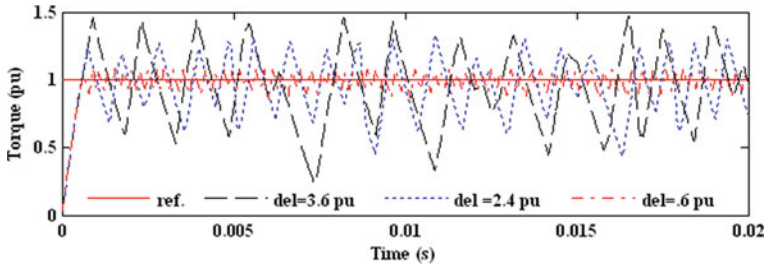

Fig. 8 Torque variation at different hysteresis bands

6.2 Torque Control Scheme with SVPWM Current Controller

SVPWM is used to regulate the torque in PMSM drives instead of a hysteresis current controller. The torque, speed, current and flux connections are all affected by changes in the carrier frequency of SVPWM. 314 rad/s is the constant speed of the PMSM drive. Figure 9 depicts the torque, speed and current responses in SVPWM with an 8 kHz carrier frequency.

As shown in Fig. 10, the third harmonic content is very high in phase current of PMSM drive at 8 kHz carrier frequency. The carrier frequency of the PMSM drive is increased to 15 and 25 kHz for analysis. Figures 11 and 13 depict the drive's reaction and from THD bar graph, i.e., Figs. 12 and 14 at these two carrier frequency shows that ripples decreases as the carrier frequency increases.

In Fig. 15, the response of torque is shown at three different values of carrier frequency, and the analyses show that the dissimilarity in torque between the actual and reference torque decreases as the carrier frequency increases in SVPWM controlled PMSM drives. Table 3 shows the level of the THD in PMSM drive considerably reduces up to the 11.32% if SVPWM technique is used in PMSM drive.

7 Conclusion

In this chapter, analysis of harmonic content in the different control strategy is done and proposed the method to reduce the content of harmonics in the control strategy

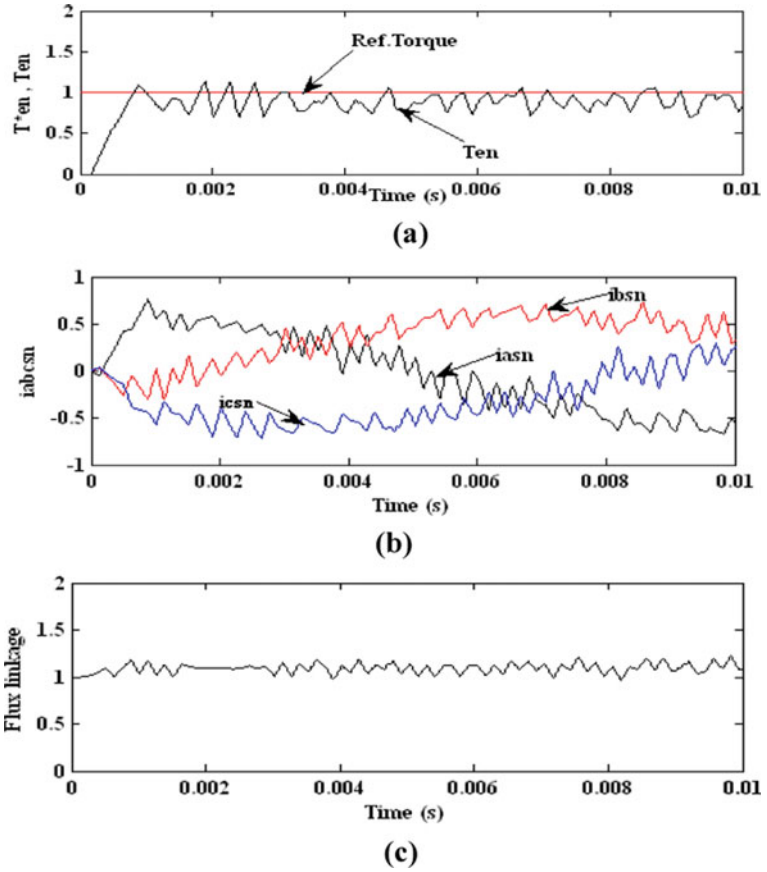

Fig. 9 With an 8 kHz carrier frequency **a** Response for torque, **b** response for phase current, **c** response for flux

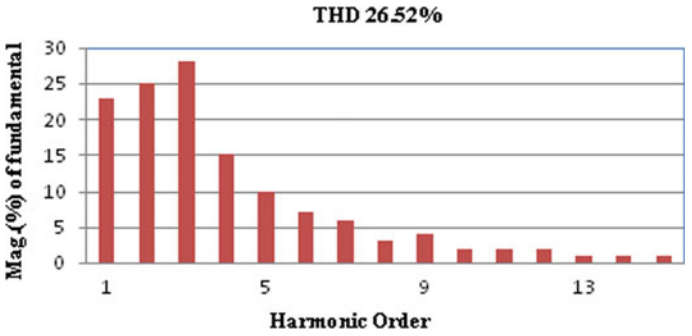

Fig. 10 THD spectrum with 8 kHz carrier frequency

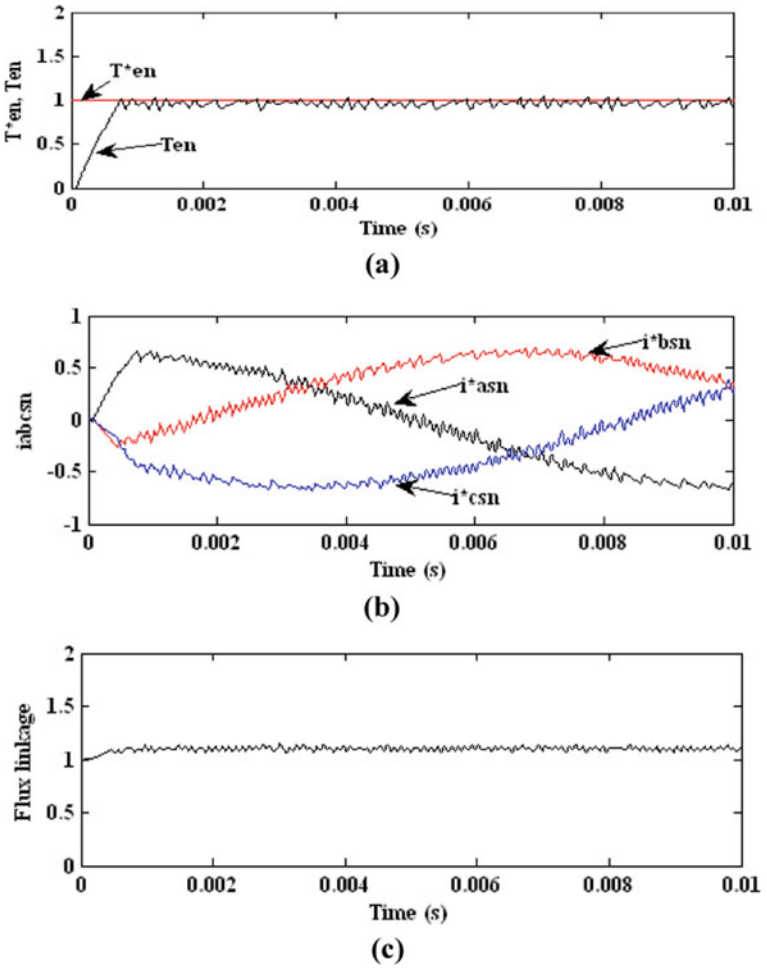

Fig. 11 With an 15 kHz carrier frequency **a** Response for torque, **b** response for phase current, **c** response for flux

of the PMSM drive. The performance of the PMSM drive improve by reducing the harmonic content and indirectly the reliability of the monitoring arrangements of the power system increase. The chapter is concluding as:

- The harmonic distortion produced by the controlling devices in the power monitoring system makes it unhealthy.
- A comparative analysis of SVPWM and hysteresis current control technique of PMSM control drive is presented in this chapter.
- THD factor calculated at different points by varying the hysteresis band and conclude it if increases the band of hysteresis the pulsation and THD factor increases in flux and torque.

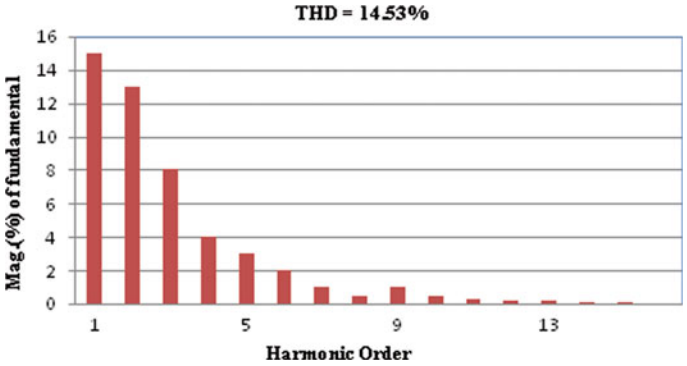

Fig. 12 THD spectrum with 25 kHz carrier frequency

- By varying the carrier frequency of SVPWM, THD factor is calculated at different levels then find it by increasing carrier frequency the pulsation and ripple in torque decreases.
- By improving the controlling system of the PMSM drive, the presentation of the drive is enhanced.
- For the application of the PMSM drive in power monitoring system, it must be high performance drive with minimum ripple factor, and also the torque pulsation is negligible.

The analyses result concluded that PMSM drive by SVPWM controller at higher carrier frequency is preferred for the application of the power monitoring system as this control drives gives the high performance with reduce ripples or torque pulsation.

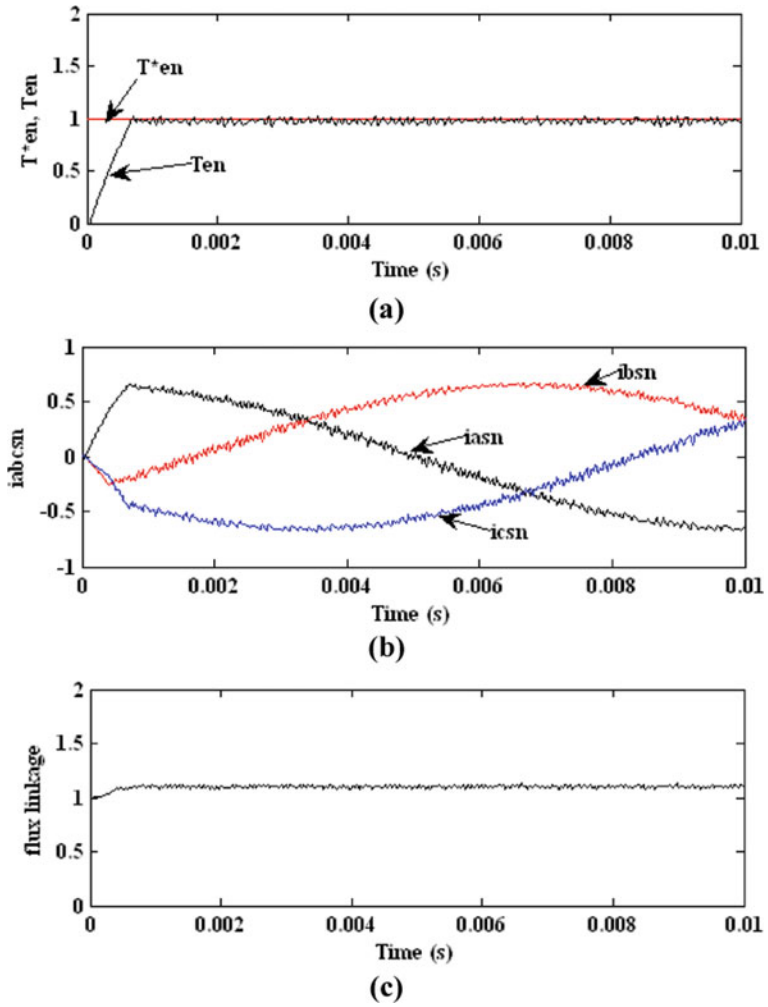

Fig. 13 With an 25 kHz carrier frequency **a** Response for torque, **b** response for phase current, **c** response for flux

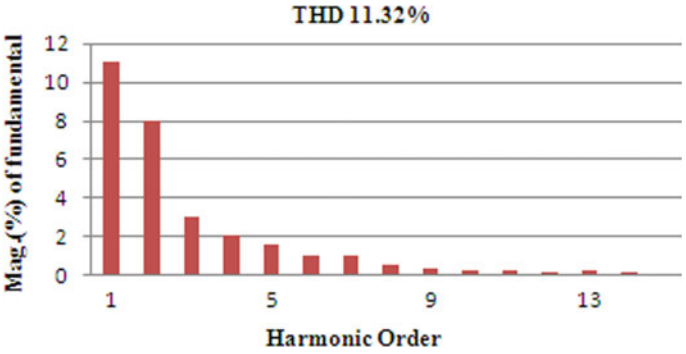

Fig. 14 THD spectrum with carrier frequency of 25 kHz

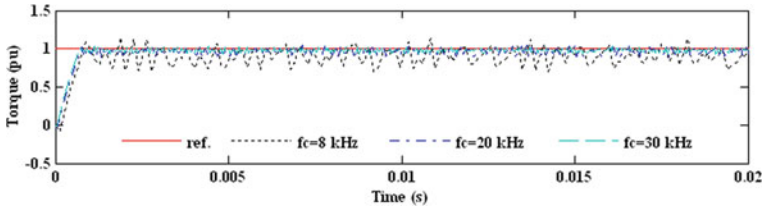

Fig. 15 Torque variation at diverse carrier frequency

Table 3 THD analysis in an SVPWM-controlled PMSM drive

S. No.	Control technique of SVPWM current	
	Carrier frequency (kHz)	THD in current (%)
1	8	26.52
2	15	14.53
3	25	11.32

References

1. G. Pellegrino, A. Vagati, B. Boazzo, P. Guglielmi, Comparison of induction and PM synchronous motor drives for EV application including design examples. IEEE Trans. Ind. Appl. **48**(6), 2322–2332 (2012). https://doi.org/10.1109/TIA.2012.2227092
2. A. Balashanmugham, M. Maheswaran, Permanent-Magnet synchronous machine drives. Mach. Electr. Mob. Solut. (2019). https://doi.org/10.5772/intechopen.88597
3. S.S. Rauth, B. Samanta, Comparative analysis of IM/BLDC/PMSM drives for electric vehicle traction applications using ANN-Based FOC, in *IEEE 17th India Council International Conference (INDICON)*, pp. 1–8 2020. https://doi.org/10.1109/INDICON49873.2020.9342237
4. A. Iqbal et al., *Renewable Power for Sustainable Growth* (Springer Nature, Part of the Lecture Notes in Electrical Engineering), vol. 723, p. 805. ISBN 978-981-33-4080-0. https://doi.org/10.1007/978-981-33-4080-0

5. N. Fatema et al., *Intelligent Data-Analytics for Condition Monitoring: Smart Grid Applications* (Academic Press, 2021). ISBN 978-0-323-85510-5. https://doi.org/10.1016/C2020-0-02173-0
6. I.M. Alsofyani, K. Lee, Predictive torque control based on discrete space vector modulation of PMSM without flux error-sign and voltage-vector lookup table. Electronics **9**, 1542 (2020). https://doi.org/10.3390/electronics9091542
7. P. Karamanakos, T. Geyer, Guidelines for the design of finite control set model predictive controllers. IEEE Trans. Power Electron. **35**(7), 7434–7450 (2020)
8. L. Tang, L. Zhong, M.F. Rahman, Y. Hu, A novel direct torque controlled interior permanent magnet synchronous machine drive with low ripple in flux and torque and fixed switching frequency. IEEE Trans. Power Electron. **19**, 346–354 (2004)
9. C. Ogbuka, M.N. Caiethna, M. Agu, A high performance hysteresis current control of a permanent magnet synchronous motor drive. Turkish J. Electr. Eng. Comput. Sci. (2017). https://doi.org/10.3906/ELK-1505-160
10. J.A. Güemes, A.M. Iraolagoitia, J.I. Del Hoyo, P. Fernandez, Torque analysis in permanent-magnet synchronous motors: a comparative study. IEEE Trans. Energy Convers **26**(1) (2011)
11. A.K. Yadav et al., *Soft Computing in Condition Monitoring and Diagnostics of Electrical and Mechanical Systems* (Springer Nature, Part of the Advances in Intelligent Systems and Computing, 2020), vol. 1096, p. 496, ISBN 978-981-15-1532-3. https://doi.org/10.1007/978-981-15-1532-3
12. R. Pindoriya, A.K. Mishra, B.S. Rajpurohit, R. Kumar, Performance analysis of control strategies of permanent magnet synchronous motor, in *IEEE Conference TENCON* (2016)
13. R. Tak, S.Y. Kumar, B.S. Rajpurohit, Modeling the torque control scheme of surface mounted permanent magnet synchronous motor. Int. J. Mech. Eng. Technol. **8**(5), 1137–1146 (2017)
14. O. Cosmas, N. Cajethan, A. Marcel, A fast hysteresis current-controlled permanent magnet synchronous motor drive based on field orientation. J. Electr. Eng. **67**(2), 69–77 (2016)
15. J.M. Lazi, Z. Ibrahim, M. Sulaiman, Mean and differential torque control using hysteresis current controller for dual PMSM drives. J. Theor. Appl. Inf. Technol. **33**(1) (2011)
16. H. Lin, T.A. Lipo, B. Kwon, S.R. Cheon, Three level hysteresis current control for a three-phase permanent magnet synchronous motor drive, in *Power Electronics and Motion Control 7th International IEEE Conference in China*, 2012
17. A. Ebrahimi, M. Maier, N. Parspour, Analysis of torque behaviour of Permanent magnet synchronous motor in field weakening operation, in *Power and Energy Conference at USA* (IEEE, 2013)
18. G. Pei, L. Li, X. Gao, J. Liu, R. Kennel, Predictive current trajectory control for PMSM at voltage limit. IEEE Access **8**, 1670–1679 (2020)
19. S. Srivastava et al., *Applications of Artificial Intelligence Techniques in Engineering—Volume 1* (Springer Nature, Part of the Advances in Intelligent Systems and Computing, 2018), vol. 698, p. 643. ISBN 978-981-13-1819-1. https://doi.org/10.1007/978-981-13-1819-1
20. Y. Miyama, M. Hazeyama, S. Hanioka, N. Watanabe, A. Daikoku, M. Inoue, PWM carrier harmonic iron loss reduction technique of permanent-magnet motors for electric vehicles. IEEE Trans. Indust. Appl. **52**(4) (2016)
21. R. Tak, S.Y. Kumar, B.S. Rajpurohit, Speed control schemes of four quadrant operating PMSM drive for electric vehicles applications. Int. J. Appl. Eng. Res. **12**(15), 5156–5162 (2017). ISSN 0973-4562
22. Tomaoz Rudnicki, Robert Czerwinski, Dariuoz Polok and Andrzej Sikora, "Performance analysis of a PMSM drive with torque and speed control" , Mixed Design of Integrated circuits and systems, 22nd IEEE International conference, 2015.
23. R. Tak, S.Y. Kumar, B.S. Rajpurohit, Dynamic modeling of surface mounted permanent synchronous motor for servo motor application. Int. J. Sci. Res. Eng. Technol. **6**(8) (2017)
24. R. Tak, S. Shukla, B.S. Rajpurohit, Performance analysis permanent magnet synchronous motor drives with pulse width modulation control technique, in *Algorithms for Intelligent Systems* (Springer). ISSN: 2524-7565